A Bidentate Bisphosphine Functioning in Intramolecular Aliphatic Metalation and as an NMR Spectroscopic Probe for the Metal Coordination Environment

William Lesueur, Euro Solari, and Carlo Floriani*

Institut de Chimie Minérale et Analytique, BCH, Université de Lausanne, CH-1015 Lausanne, Switzerland

Angiola Chiesi-Villa and Corrado Rizzoli

Dipartimento di Chimica, Università di Parma, I-43100 Parma, Italy

Received January 23, 1997[⊗]

The multistep synthesis of the novel diphosphine reference ligand L_2, **6**, $Ph_2P(o\text{-}C_6H_4CH_2C_6H_4\text{-}o)PPh_2$, has been streamlined and can be prepared on a *ca.* 20 g scale. It forms metallacycles with a variety of metal fragments. The resulting, and very rigid, boat−boat conformation forces a proton (H_{endo}) of the bridging methylene in close proximity to the metal, which in turn renders these protons (H_{endo}, H_{exo}) diastereotopic. The NMR spectra of $[L_2MCl_2]$ [M = Pd, **9**; M = Pt, **10**] and of the organometallic derived compounds $[L_2Pd(PPh_3)]$, **11**, and $[L_2Pd(Cl)(\eta^2\text{-}CH_2Ph)]$, **12**, consist of a pair of doublets, with the H_{endo} coupled to the P of the metallacycle. The CH_2−metal close proximity drives the electrophilic metalation of the bridging methylene by $RhCl_3$ to form $[L^*_2Rh(Cl)_2(MeCN)]$, **13**, [$L^*_2 = Ph_2P(o\text{-}C_6H_4CHC_6H_4\text{-}o)PPh_2$]. A significant example, which shows how the coordination number of the metal can affect the H_{exo}−H_{endo} resonance separation, is provided by the couple $[L_2Ni(C_2H_4)]$, **14**, and $[L_2Ni(CO)_2]$, **15**. In order to show that the metallacycle size is crucial for the bridging methylene to function as a spectroscopic probe, we complexed the same $[Fe(CO)_3]$ fragment to L_2, **6**, and L'_2, **17**, [$L'_2 = Ph_2PO(o\text{-}C_6H_2(4,6Bu^t_2)CH_2(4,6Bu^t_2)C_6H_2\text{-}o)OPPh_2$], to give $[L_2Fe(CO)_3]$, **19**, and $[L'_2Fe(CO)_3]$, **18**, respectively. In complex **17** the diastereotopic nature of these protons and hence the spectroscopic information was lost because of the presence of a 10-membered metallacycle. Crystal data: **9** is triclinic, space group $P\bar{1}$, $a = 11.987(1)$ Å, $b = 15.990(2)$ Å, $c = 10.872(1)$ Å, $\alpha = 91.42(1)°$, $\beta = 111.01(2)°$, $\gamma = 99.86(2)°$, $V = 1908.2(5)$ Å^3, $Z = 2$, and $R = 0.053$; **11** is monoclinic, space group $C2/c$, $a = 39.071(5)$ Å, $b = 13.657(4)$ Å, $c = 19.848(5)$ Å, $\beta = 92.45(2)°$, $V = 10581(5)$ Å^3, $Z = 8$, and $R = 0.047$; **12** is triclinic, space group $P\bar{1}$, $a = 11.289(1)$ Å, $b = 18.769(2)$ Å, $c = 11.077(1)$ Å, $\alpha = 91.20(1)°$, $\beta = 111.27(1)°$, $\gamma = 105.26(1)°$, $V = 2107.7(4)$ Å^3, $Z = 2$, and $R = 0.039$; **13** is orthorhombic, space group $P2_12_12_1$, $a = 15.346(2)$ Å, $b = 18.188(3)$ Å, $c = 12.072(2)$ Å, $V = 3369.5(9)$ Å^3, $Z = 4$, and $R = 0.042$.

Introduction

The bidentate bisphosphine derivatives in their achiral and chiral form are the ligands "par excellence" in coordination, organometallic chemistry, and catalysis.[1,2] They have been proposed in a variety of forms. This report deals with a diphosphine having the following particular skeleton:

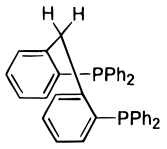

$L_2 = [Ph_2P\text{-}(o\text{-}C_6H_4\text{-}CH_2\text{-}C_6H_4\text{-}o)\text{-}PPh_2]$

There are a number of features associated with this type of skeleton: (i) It is the monomeric fragment of the cyclic oligomeric calix[*n*]arenes.[3] (ii) The eight-membered derived metallacycle has a very rigid conformation and, in spite of the rather large ring size, a narrow P···P bite. (iii) The rigid boat−boat conformation, observed for all the complexes so far identified, forces the *endo* hydrogen of the bridging methylene to approach the metal and consequently can favor the observed metalation of the methylene group. Further, this type of intramolecular C−H activation in diphosphine complexes, as elucidated by Shaw,[4] Milstein,[5] and others, can be promising in driving the intermolecular hydrocarbon activation.[5] (iv) The metal complexation by the reference ligand affords a conformationally rigid metallacycle which easily differentiates the prochiral methylene protons (in the free ligand). The *endo* one is affected by the proximity to the metal and by other electronic

* To whom correspondence should be addressed.

⊗ Abstract published in *Advance ACS Abstracts*, July 1, 1997.

(1) (a) McAuliffe, C. A. Phosphorus, Arsenic, Antimony and Bismuth Ligands. In *Comprehensive Coordination Chemistry*; Wilkinson, G., Gillard, R. D., McCleverty, J. A., Eds.; Pergamon: Oxford, U.K., 1987; Vol. 2, p 989. (b) *Homogeneous Catalysis with Metal Phosphine Complexes*; Pignolet, L. H., Ed.; Plenum: New York, 1983. (c) Puddephatt, R. J. *Chem Soc. Rev.* **1983**, *12*, 99. (d) Levason, W. *The Chemistry of Organophosphorus Compounds*; Hartley, F. R., Patai, S., Eds.; Wiley: New York, 1990; Vol. 1; p 617. Stelzer, O.; Langhans, K.-P. *Ibid.*, p 191. (e) Cotton, F. A.; Hong, B. *Progr. Inorg. Chem.* **1992**, *40*, 179. (f) Mayer, H. A.; Kaska, W. C. *Chem. Rev.* **1994**, *94*, 1239.

(2) (a) For a comprehensive review on chiral phosphorus ligands see: Brunner, H.; Zettlmaier, W. *Handbook of Enantioselective Catalysis*; VCH: Weinheim, Germany, 1993; Vols. I, II. (b) Pietrusiewicz, K. M.; Zablocka, M. *Chem. Rev.* **1994**, *94*, 1375. (c) Herrmann, W.; Kohlpaintner, C. W. *Angew. Chem., Int. Ed. Engl.* **1993**, *32*, 1524 and references therein.

(3) (a) Gutsche, C. D. *Calixarenes*; The Royal Society of Chemistry: Cambridge, U.K., 1989. (b) *Calixarenes, A Versatile Class of Macrocyclic Compounds*; Vicens, J., Böhmer, V., Eds.; Kluwer: Dordrecht, The Netherlands, 1991.

(4) Empsall, H. D.; Hyde, E. M.; Markham, R.; McDonald, W. S.; Norton, M. C.; Shaw, B. L.; Weeks, B. *J. Chem. Soc., Chem. Commun.* **1977**, 589. Crocker, C.; Errington, R. J.; Markham, R.; Moulton, C. J.; Shaw, B. L. *J. Chem. Soc., Dalton Trans.* **1982**, 387.

S0020-1669(97)00081-5 CCC: $14.00

and magnetic field affects and thus functions as a very sensitive NMR spectroscopic probe for the metal environment. In this context we will show how enlargement to a 10-membered metallacycle causes the loss in conformation control and, consequently, loss of the ability of CH_2 to act as a spectroscopic probe in NMR analyses.

Herein we report an improved and scaled up synthesis of the reference ligand along with its use in the complexation of a variety of metal fragments. In particular we have focused on the complexation of $PdCl_2$ and its organometallic derivatization and the electrophilic metalation of the bridging methylene by $RhCl_3$. Further we show how a change in the coordination number of the metal can affect the chemical shift of the *endo* proton, exemplified with some Ni^0 derivatives, and how enlarging the metallacycle to a 10-membered ring results in loss of the spectroscopic probe ensured by the bridging methylene. This has been shown using both L_2 and L'_2 derived species.

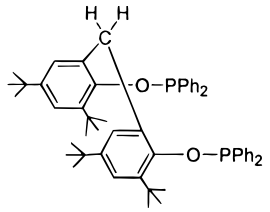

L'2, [Ph_2P-O-(*o*-C_6H_2(4,6Bu^t_2)-CH_2-(4,6Bu^t_2)C_6H_2-*o*)-O-PPh_2]

In preliminary studies we showed how the bridging methylene of the bis-phenolato anion precursor of L'_2 can be used as an NMR spectroscopic probe.[6] In order to support the fundamental assumption on the rigidity of the metallacycle conformation in a variety of complexes derived from L_2, X-ray analyses have been carried out on the key complexes. This allowed, among other things, the establishment of a structural solid state−solution relationship.

Experimental Section

General Procedure. All reactions were carried out under an atmosphere of purified nitrogen. Solvents were dried and distilled before use by standard methods. Infrared spectra were recorded with a Perkin-Elmer 883 spectrophotometer; ^{1}H, ^{31}P, and ^{13}C NMR spectra were measured on a 200-AC Bruker instrument at 298 K, unless specified. Compounds **1** and **16** are commercially available.

Preparation of 2.[7] (2-aminophenyl)phenylmethane (50.4 g, 270 mmol) was dissolved of in a mixture of 32% HCl (109 mL) and water (60 mL) and the mixture cooled at 0 °C. A solution of $NaNO_2$ (20.5 g) in water (85 mL) was added in small volumes of 2−3 mL (the temperature was not allowed to rise above 10 °C). After 30 min a solution of KI (46.0 g) in water (50 mL) was added dropwise with the concomitant evolution of N_2 gas (again, the temperature was not allowed to rise above 10 °C). The mixture was warmed to room temperature and then to 60 °C until effervescence ceased. After cooling, the upper aqueous layer was decanted and the organic layer washed with 10% NaOH solution. A small amount of $Na_2S_2O_5$ (*ca.* 0.5 g) was added until the crude reaction mixture was a pale red color. This mixture was steam distilled in order to eliminate final traces of unreacted amine. The aqueous layer was eliminated, the organic residue distilled (Vigreux 8 cm), and the fraction (bp: 125−126 °C, ∼10^{-2} Torr) collected (colorless when hot, red on cooling) (lit. bp: 110−111 °C/0.01 mmHg, or 175−180 °C/14−17 mmHg, or 177 °C/12 mmHg) to give **2** (70%). n_D^{28}: 1.637 (lit.: $n_D^{22.5}$ 1.6417 or n_D^{20} 1.6406). ^{1}H-NMR (CCl_4, TMS): δ 4.06 (s, 2H, CH_2), 6.70−7.91 (m, 9H, Ar-*H*). Mass EI: *m*/*z* 294 (calcd: 294.13).

Preparation of 3.[8] A solution of peracetic acid[9] was prepared by slowly adding 30% H_2O_2 (77 mL) to acetic anhydride (308 mL) at 0 °C. The mixture was kept cold in an ice-water bath until it became homogeneous and then left to stand overnight at room temperature. A solution of **2** (57.0 g, 100 mmol) dissolved in acetic acid (60 mL) was added dropwise over 2 h to the peracetic acid solution at 10 °C. The mixture slowly turned from orange to yellow and was allowed to stand at room temperature for 4 days. The reaction mixture (which now contains the iodoso compound) was cooled to 10 °C, and to this stirred solution was added dropwise 96% H_2SO_4 (77 mL). The mixture became dark and after standing for 12 h at room temperature was diluted with of cold water (200 mL), extracted with toluene (200 mL), treated with activated carbon until the solution was colorless, and then treated with a large excess of NaCl. Filtration yielded **3** as a white powder (73%). Mp: 245 °C (lit.: 244−245 °C). ^{1}H NMR (DMSO-d_6): δ 4.23 (s, 2H, CH_2), 7.35 (d t, 2H, Ar-H_γ), 7.52 (dt, 2H, Ar-H_β) 7.72 (dd, 2H, Ar-H_δ), 8.22 (dd, 2H, Ar-H_α). Anal. Calcd for $C_{13}H_{10}ClI$: C, 47.52; H, 3.07. Found: C, 48.01; H, 2.99.

Preparation of 4.[8] A mixture of **3** (45.4 g, 138 mmol), water (200 mL), ethanol (200 mL), and KI (excess) was refluxed for 15 min. The off-white precipitate was collected by filtration and dried in a desiccator over $CaCl_2$ for 2 days (99%). MP: 198−199 °C (lit.: 184.5−185.5 or 177−178 °C). ^{1}H NMR (DMSO-d_6): δ 4.23 (s, 2H, CH_2), 7.35 (d t, 2H, Ar-H_γ), 7.52 (d t, 2H, Ar-H_β), 7.72 (d d, 2H, Ar-H_δ), 8.22 (d d, 2H, Ar-H_α). Anal. Calcd for $C_{13}H_{10}I_2$: C, 37.17; H, 2.40; I, 60.43. Found: C, 36.89; H, 2.37; I, 59.30.

Preparation of 5.[10] **4** (49.2 g, 120 mmol) was heated under N_2 at 210 °C for 15 min. After cooling, the resulting violet liquid was dissolved in CH_2Cl_2 (150 mL) and washed with an aqueous solution of $Na_2S_2O_3$. The organic layer was then dried ($MgSO_4$), the solvent removed, and then the solid recrystallized in diethyl ether (69%). Mp: 78 °C (lit.: 79 °C). ^{1}H NMR (CD_2Cl_2): δ = 4.13 (s, 2H, CH_2), 6.95 (m, 4H, Ar-*H*), 7.27 (m, 2H, Ar-*H*), 7.85 (m, 2H, Ar-*H*). Anal. Calcd for $C_{13}H_{10}I_2$: C, 37.17; H, 2.40; I, 60.43. Found: C, 36.89; H, 2.28; I, 61.20. Mass EI: *m*/*z* 420 (calcd: 420.04).

Preparation of Ph_2P(*o*-$C_6H_4CH_2C_6H_4$-*o*)PPh_2, L_2, 6. Bu^nLi (1.6 M in hexane, 29.8 mL, 47.6 mmol) was added dropwise to a stirred suspension of **5** (10.0 g, 23.8 mmol) in pentane (80 mL) at room temperature. After 2 h, freshly distilled chlorodiphenylphosphine (10.50 g, 47.6 mmol) was added to the chilled (0 °C) yellow suspension. The mixture turned orange. After 5 days at room temperature, the mixture was hydrolyzed with an aqueous saturated solution of NH_4Cl. The aqueous layer was eliminated, and the pale yellow suspension in the organic layer was collected by filtration and washed with a minimum of cold methanol. The white solid was dried *in vacuo* for 8 h (73%). Mp: 128−129 °C. ^{1}H NMR (CD_3COCD_3): δ = 4.45 (brd t, 2 H, J_{PH} = 2.0 Hz, CH_2), 6.87−7.36 (m, 28 H, Ar-*H*). ^{31}P{^{1}H} NMR (CD_3COCD_3): δ = −11.5 (s). Anal. Calcd for $C_{37}H_{30}P_2$: C, 82.82; H, 5.64. Found: C, 82.15; H, 5.63.

Preparation of L_2NiCl_2, 7.[11] A mixture of $NiCl_2 \cdot 6H_2O$ (0.81 g, 2.8 mmol) and L_2, **6** (1.5 g, 2.8 mmol), in ethanol was refluxed for 3 h. The mixture was allowed to cool to room temperature and the khaki microcrystalline powder collected by filtration and dried (75%). Anal. Calcd for $C_{37}H_{30}Cl_2NiP_2$: C, 66.71; H, 4.54; Cl, 10.65. Found: C, 66.32; H, 4.32; Cl, 9.95. μ_{eff}: 3.30 μ_B (298 K).

(5) (a) Milstein, D. Frontiers in Bond Activation by Electron-Rich Metal Complexes. In *Stereoselective Reactions of Metal-Activated Molecules*; Werner, H., Sundermeyer, J., Eds.; Vieweg: Braunschweig/Wiesbaden, Germany, 1995; pp 107−115. (b) Gozin, M.; Weisman, A.; Ben-David, Y.; Milstein, D. *Nature* **1993**, *364*, 699. (c) Gozin, M.; Aizenberg, M.; Liou, S.-Y.; Weisman, A.; Ben-David, Y.; Milstein, D. *Nature* **1994**, *370*, 42.

(6) Lesueur, W.; Corazza, F.; Floriani, C.; Chiesi-Villa, A.; Guastini, C. *Angew. Chem., Int. Ed. Engl.* **1989**, *28*, 66.

(7) Seidel, F. *Ber.* **1928**, *61*, 2267.

(8) Collette, J.; McGreer, D.; Crawford, R.; Chubb, F.; Sandin, R. B. *J. Am. Chem. Soc.* **1956**, *78*, 3819.

(9) For an excellent review wich contains valuable information on the preparation of organic peracids and precautions necessary in their use, see: Swern, D. *Organic Reactions*; Wiley: New York, 1953; Vol. VII, p 378.

(10) (Bickelhaupt, F.; Jongsma, C.; de Koe, P.; Lourens, R.; Mast, N. R.; van Mourik, G. L.; Vermeer, H.; Weustink, R. J. M. *Tetrahedron* **1976**, *32*, 1921.

(11) Following the procedure by: Colquhoum, H. M.; Holton, J.; Thompson, D. J.; Twigg, M. V. *New pathways for organic synthesis, practical applications of transitions metals*; Plenum: New York, 1984; Chapter 9.

Preparation of L_2NiBr_2, 8. A mixture of $NiBr_2 \cdot 3H_2O$ (0.762 g, 2.79 mmol) and L_2, **6** (1.5 g, 2.8 mmol), in ethanol was refluxed for 3 h. The mixture was allowed to cool at room temperature and the deep green microcrystalline powder collected by filtration and dried (70%). Anal. Calcd for $C_{37}H_{30}Br_2NiP_2$: C, 58.85; H, 4.00. Found: C, 58.89; H, 3.95. μ_{eff}: 3.40 μ_B (298 K).

Preparation of L_2PdCl_2, 9. An equimolar mixture of $[PdCl_2(PhCN)_2]$[12] (2.00 g, 5.22 mmol) and L_2, **6** (2.80 g, 5.20 mmol), was refluxed for 3 h in benzene (100 mL) and then cooled to room temperature. The pale yellow solid was filtered out, washed with benzene and ether, and dried *in vacuo* for 4 h (88%). ^{1}H NMR (CD_2Cl_2): δ 3.84 (d, 1H, J_{H-H} = 14 Hz, C*H*$_2$), 6.56 (brd d, 1H, J_{HH} = 14 Hz, *CH*$_2$), 6.70−7.68 (m, 28H, Ar-*H*). ^{31}P{^{1}H} NMR (CD_2Cl_2, ppm): δ 23.4 (s). Anal. Calcd for $C_{37}H_{30}Cl_2P_2Pd$: C, 62.25; H, 4.24; Cl, 9.93. Found: C, 61.93; H, 4.32; Cl, 9.72.

Preparation of L_2PtCl_2, 10. A solution of K_2PtCl_4 (1.54 g, 3.72 mmol) in the minimum amount of water/ethanol (1:2) was added to a solution of L_2, **6** (2.00 g, 3.72 mmol), in CH_2Cl_2 (30 mL). The mixture was refluxed for 12 h. After the mixture was cooled to room temperature, the pale yellow solid was collected by filtration and dried *in vacuo* (78%). ^{1}H NMR (CD_2Cl_2): δ 3.44 (d, 1H, J_{HH} = 14 Hz, *CH*$_2$), 6.46 (brd d, 1H, J_{HH} = 14 Hz, *CH*$_2$), 6.52−6.61 (m, 2H, Ar-*H*), 6.79−6.86 (m, 2H, Ar-*H*), 7.18−7.62 (m, 24H, Ar-*H*). ^{31}P{^{1}H} NMR (CD_2Cl_2): δ 3.55 (t, J_{Pt-P} = 3.686 Hz). Anal. Calcd for $C_{37}H_{30}Cl_2P_2Pt$: C, 55.37; H, 3.77; Cl, 8.84. Found: C, 54.89; H, 3.84; Cl, 8.42.

Preparation of $[L_2Pd(PPh_3)]$, 11. A mixture of L_2PdCl_2, **9** (0.53 g, 0.73 mmol), and PPh_3 (0.50 g, 1.9 mmol) in DMSO (15 mL) was heated until the solution became clear orange. To this was added $N_2H_4 \cdot H_2O$ (0.15 mL, 3.0 mmol). A vigorous evolution of gas was observed, and the color turned yellow. The solution was immediately cooled in an ice-water bath, resulting in yellow crystals. These crystals were filtered out, washed with ethanol (O_2 free), and then dried *in vacuo* for 4 h (64%). ^{1}H NMR (C_6D_6): δ 3.08 (d, 1H, J_{HH} = 14 Hz, *CH*$_2$), 6.15 (d, 1H, J_{HH} = 14 Hz, *CH*$_2$), 6.37−7.48 (m, 39H, Ar-*H*), 7.92 (brd s, 4H, Ar-*H*). ^{31}P{^{1}H} NMR (C_6D_6): δ 6.78 (s), 23.94 (s). Anal. Calcd for $C_{55}H_{45}P_3Pd$: C, 72.97; H, 5.01. Found: C, 72.58; H, 5.21.

Preparation of $[L_2Pd(Cl)(\eta^2\text{-}CH_2Ph)]$, 12. A mixture of $[L_2Pd(PPh_3)]$, **11** (0.39 g, 0.43 mmol), and freshly distilled benzyl chloride (0.05 mL, 0.43 mmol) in toluene (15 mL) was heated at 80 °C for 10 min. The color turned from yellow to orange red. Cooling to room temperature and standing at 4 °C for 12 h yielded red crystals of **12** (80%). ^{1}H NMR (CD_2Cl_2): δ 2.80 (brd s, 1H, *CH*$_2$ *benzyl*), 3.25 (d, 1H, J_{HH} = 15 Hz, *CH*$_2$), 4.00 (brd s, 1H, *CH*$_2$ *benzyl*), 6.20−8.00 (m, 34H, Ar-*H* and C*H*$_2$). ^{31}P{^{1}H} NMR (C_6D_6): δ 9.58 (s), 27.71 (s). Anal. Calcd for **12**$\cdot C_7H_8$, $C_{51}H_{45}ClP_2Pd$: C, 71.08; H, 5.26; Cl, 4.11. Found: C, 71.58; H, 5.37; Cl, 3.80.

Preparation of $[L^*_2Rh(Cl)_2(MeCN)]$, 13 [L^*_2 = $Ph_2P(o\text{-}C_6H_4CHC_6H_4\text{-}o)PPh_2$]. A red ethanolic solution of $RhCl_3 \cdot 2H_2O$ (0.23 g, 0.93 mmol) was added to a solution of L_2, **6** (0.50 g, 0.93 mmol), in ethanol/acetonitrile (1:1), which was then refluxed for 30 min. To this hot mixture was added an aqueous solution of formaldehyde (36.5%, 2 mL). This mixture was refluxed for 4 h and then cooled slowly to room temperature to give a murky yellow solution. The solution was filtered and the filtrate kept at room temperature overnight. The deep yellow crystals were collected and washed with Et_2O (82.6%). IR (KBr/Nujol): ν(CN), 1969 cm^{-1}. ^{1}H NMR (CD_3OD): δ 6.5−6.8 (m, 5H), 7.1−7.8 (m, 20H), 7.9−8.1 (m, 4H). ^{31}P{^{1}H}NMR (CD_3OD): δ 60.3 (d, J_{Rh-P} = 145 Hz), 54.60 (d, J_{Rh-P} = 143 Hz). Anal. Calcd for $C_{39}H_{32}Cl_2NP_2Rh$: C, 62.42; H, 4.30; N, 1.87. Found: C, 63.14; H, 4.52; N, 1.67.

Preparation of $[L_2Ni(C_2H_4)]$, 14.[13] To a green suspension of anhydrous $[Ni(C_5H_7O_2)_2]$ (1.10 g, 4.29 mmol) in toluene (80 mL) at room temperature was added L_2, **6** (2.30 g, 4.29 mmol, 1 equiv). Ethylene was bubbled into this mixture for 5 min and then a hexane solution of $Al(Et)_3$ (2 equiv) carefully added. The solution became first yellow-orange and then orange-red after 3 h. Methanol (150 mL, O_2 free) was added. The mixture was filtered and the filtrate kept at 4 °C for 12 h, to give green khaki microcrystalline **14** (67%). ^{1}H NMR (C_6D_6): δ 3.49 (d, 1H, J_{HH} = 14.4 Hz, *CH*$_2$), 6.60−7.47 (m, 33H, Ar-*H*, C_2H_4, C*H*$_2$). ^{31}P{^{1}H} NMR (C_6D_6): δ 22.7 (s). Anal. Calcd for $C_{39}H_{34}NiP_2$: C, 75.15; H, 5.50. Found: C, 74.87; H, 5.42. IR (Nujol): ν(C_2H_4), 1520 cm^{-1}.

Preparation of $[L_2Ni(CO_2)]$, 15. To a yellow suspension of $[L_2Ni(C_2H_4)]$, **14**, in degassed methanol (30 mL) at room temperature was bubbled CO. The color quickly became colorless followed by precipitation of a white solid. The solid was collected by filtration and dried *in vacuo* for 2 h to give **15** as a pale gray powder (45%). ^{1}H-NMR (CD_2Cl_2): δ 3.42 (d, 1H, J_{HH} = 13.4 Hz, *CH*$_2$), 5.91 (d, 1H, J_{HH} = 13.4 Hz, *CH*$_2$), 6.43 (brd t, 2H, Ar-*H*), 6.81 (brd t, 2H, Ar-*H*), 7.19 + 7.39 (brd s, 24H, Ar-*H*). ^{31}P{^{1}H} NMR (CD_2Cl_2): δ 24.8 (s). Anal. Calcd for $C_{39}H_{30}NiO_2P_2$: C, 71.92; H, 4.64. Found: C, 71.46; H, 4.70. IR (KBr/Nujol): ν(CO), 1991 (s), 1925 (s) cm^{-1}.

Preparation of $Ph_2PO(o\text{-}C_6H_2(4,6Bu^t_2)CH_2(4,6Bu^t_2)C_6H_2\text{-}o)OPPh_2$, L′$_2$, 17. To a *n*-hexane (70 mL) solution of **16** (3.40 g, 8.0 mmol) was added a solution of Bu^nLi (1.6 M, 16 mmol) in *n*-hexane. After 30 min, 2 equiv of freshly distilled $ClPPh_2$ (3.0 mL, 16 mmol) was added at room temperature. After 13 h, the solid was removed by filtration and the filtrate evaporated to dryness. The resulting white solid was dried *in vacuo* (84%). ^{1}H NMR (CD_2Cl_2): δ 1.08 (s, 18H, *p*-Bu^t), 1.26 (s, 18H, *o*-Bu^t), 4.09 (brd t, 2H, C*H*$_2$), 6.59 (2s, 2H, Ar-*H*), 7.15 (2s, 2H, Ar-*H*), 7.29−7.46 (m, 20 H, P-Ar-H). ^{31}P{^{1}H} NMR (CD_2Cl_2): δ 113.5 (s). Anal. Calcd for $C_{53}H_{62}O_2P_2$: C, 80.27; H, 7.88. Found: C, 79.91; H, 7.98.

Preparation of $[L'_2Fe(CO)_3]$, 18. Ligand **17** (L′$_2$) (2.4 g, 3.0 mmol) was added at −30 °C to a yellow *n*-hexane (50 mL) solution of $[Fe(CO)_3(C_8H_{14})_2]$[14] (1.08 g, 3.0 mmol) and cyclooctene (1 mL). The solution was warmed to room temperature and then was kept in the freezer for several days. A yellow crystalline solid (87%) was filtered out and dried. ^{1}H NMR (CD_2Cl_2): δ 1.07 (2s, 36H, Bu^t), 4.71 (brd s, 2H, C*H*$_2$), 6.21 (2s, 2H, Ar-*H*), 7.17−7.36 (m, 14 H, Ar-*H*), 7.54−7.58 (m, 8 H, Ar-*H*). ^{31}P{^{1}H} NMR: δ 172 (s). Anal. Calcd for $C_{56}H_{62}FeO_5P_2$: C, 72.10; H, 6.70. Found: C, 72.53; H, 6.62. IR (KBr/Nujol): ν(CO), 2008 (s), 1938 (vs), 1915 (vs) cm^{-1}.

Preparation of $[L_2Fe(CO)_3]$, 19. To a suspension of L_2, **6** (1.2 g, 2.2 mmol), in 60 mL hexane (+1 mL of cyclooctene) at −90 °C was added cold $[Fe(CO)_3(C_8H_{14})_2]$[14] (0.80 g, 2.2 mmol), and the mixture was allowed to warm slowly to room temperature (the color became red-brown at *ca.* −30 °C). This mixture was refluxed at 80 °C for 3 h. The suspension was filtered at 50 °C and then washed with Et_2O (50 mL) and dried *in vacuo* for 3 h. The crude mixture (0.79 g) was passed down a column (25 cm, 2 cm diameter) of alumina (neutral, standard grade), previously washed with benzene, eluting with a mixture of benzene/diethyl ether (1:1). The yellow fraction was collected and evaporated to dryness to give **19** as a bright yellow solid (45%). ^{1}H NMR (CD_2Cl_2): δ 3.28 (d, 1H, J_{HH} = 14 Hz, *CH*$_2$), 5.83 (d, 1H, J_{HH} = 14 Hz, *CH*$_2$), 6.31−6.40 (m, 2H, Ar-*H*), 6.68−6.76 (m, 2H, Ar-*H*), 6.98−7.38 (m, 24H, Ar-*H*). ^{31}P{^{1}H} NMR (CD_3COCD_3): δ 56.8 (s). Anal. Calcd for $C_{40}H_{30}FeP_2O_3$: C, 71.02; H, 4.47. Found: C, 71.83; H, 4.67. IR (KBr/Nujol): ν(CO), 1984 (s), 1909 (s), 1890 (s) cm^{-1}, as for C_{2v} symmetry ($2A_1 + B_2$).

X-ray Crystallography for Complexes 9 and 11−13. Suitable crystals were mounted in glass capillaries and sealed under nitrogen. The reduced cells were obtained with the use of TRACER.[15] Crystal data and details associated with data collection are given in Tables 1 and S1. Data were collected at room temperature (295 K) on a single-crystal diffractometer (Siemens AED for **9** and **12** and Rigaku for **11** and **13**). For intensities and background individual reflection profiles were analyzed.[16] The structure amplitudes were obtained after the usual Lorentz and polarization corrections,[17] and the absolute scale was established by the Wilson method.[18] The crystal quality was tested by

(12) Tsuji, J. *Organic synthesis with palladium compounds*; Springer: Berlin, Germany; Vol. 10, pp 2−3.
(13) Wilke, G.; Hermann, G. *Angew. Chem.* **1962**, *74*, 693.
(14) Fleckner, H.; Grevels, F.-W.; Hess, D. *J. Am. Chem. Soc.* **1984**, *106*, 2027.
(15) Lawton, S. L.; Jacobson, R. A. *TRACER (a cell reduction program)*; Ames Laboratory, Iowa State University of Science and Technology: Ames, IA, 1965.
(16) Lehmann, M .S.; Larsen, F. K. *Acta Crystallogr., Sect. A: Cryst. Phys., Diffr., Theor. Gen. Crystallogr.* **1974**, *A30*, 580−584.
(17) Data reduction was carried out on an IBM AT personal computer equipped with an INMOS T800 transputer.
(18) Wilson, A. J. C. *Nature* **1942**, *150*, 151.

Table 1. Experimental Data for the X-ray Diffraction Studies on Crystalline Complexes **9** and **11**−**13**

	complex			
	9	**11**	**12**	**13**
chem formula	$C_{37}H_{30}Cl_2P_2Pd\cdot 2CH_2Cl_2$	$C_{55}H_{45}P_3Pd\cdot 1.5C_6D_6$	$C_{44}H_{37}ClP_2Pd\cdot C_7H_8$	$C_{39}H_{32}Cl_2NP_2Rh$
a (Å)	11.987(1)	39.071(5)	11.289(1)	15.346(2)
b (Å)	15.990(2)	13.657(4)	18.769(2)	18.188(3)
c (Å)	10.872(1)	19.848(5)	11.077(1)	12.072(2)
α (deg)	91.42(1)	90	91.20(1)	90
β (deg)	111.01(2)	92.45(2)	110.27(1)	90
γ (deg)	99.86(2)	90	105.26(1)	90
V (Å)^3	1908.2(5)	10581(4)	2107.7(4)	3369.5(9)
Z	2	8	2	4
fw	883.8	1022.5	861.7	750.4
space group	$P\bar{1}$ (No. 2)	*C*2/*c* (No. 15)	$P\bar{1}$ (No. 2)	$P2_12_12_1$ (No. 19)
t (°C)	22	22	22	22
λ (Å)	1.541 78	0.710 69	1.541 78	0.710 69
ρ_{calcd} (g cm^{-3})	1.538	1.284	1.358	1.479
μ (cm^{-1})	90.18	4.72	52.10	7.80
transmn coeff	0.744−1.000	0.957−1.000	0.590−1.000	0.745−1.000
R	0.053	0.047	0.039	0.042 [0.043][a]
*wR*2	0.143	0.127	0.103	0.127 [0.130]
GOF	1.034	0.828	1.021	0.852

[a] Values in brackets refer to the "inverted structure". $R = \sum|\Delta F|/\sum|F_o|$ based on the unique observed data. $wR2 = [\sum w|\Delta F^2|^2/\sum w|F_o^2|^2]^{1/2}$ based on the unique observed data for **9** and **12** and on the unique total data for **11** and **14**. GOF $= [\sum w|\Delta F^2|^2/(NO - NV)]^{1/2}$.

ψ scans showing that crystal absorption effects could not be neglected. The data were corrected for absorption using ABSORB[19] for complexes **9** and **12** and a semiempirical method[20] for complexes **11** and **13**. The function minimized during the least-squares refinement was $\sum w(\Delta F^2)^2$. Weights were applied according to the scheme $w = 1/[\sigma^2(F_o)^2 + (aP)^2]$ ($P = (F_o^2 + 2F_c^2)/3$) with $a = 0.1011$, 0.0463, 0.0678, and 0.1041 for complexes **9** and **11**−**13**, respectively. Anomalous scattering corrections were included in all structure factor calculations.[21b] Scattering factors for neutral atoms were taken from ref 21a for nonhydrogen atoms and from ref 22 for H. Among the low-angle reflections no correction for secondary extinction was deemed necessary. All calculations were carried out on an IBM PS2/80 personal computer and on an ENCORE 91 computer. The structures were solved by the heavy-atom method starting from three-dimensional Patterson maps using the observed reflections. Structure refinements were carried out using SHELX92[23] and based on the unique total data for **11** and **13** and on the unique observed data for **9** and **12**. Refinement was first done isotropically and then anisotropically for all non-H atoms except for the disordered atoms. Refinements of complexes **12** and **13** were straightforward. In complex **9** one of the two CH_2Cl_2 solvent molecule of crystallization was found to be affected by disorder which was solved by splitting the carbon and chlorine atoms over three positions (A, B, C) isotropically refined with site occupation factors of 0.5, 0.25, and 0.25, respectively. During the refinement the C−Cl bond distances were constrained to be 1.75(1) Å. In complex **11** a C_6D_6 solvent molecule of crystallization was found to be disordered over two positions (A, B) rotated each other by about 30°. They were isotropically refined with a site occupation factor of 0.5 constraining the aromatic rings to be regular hexagons (C−C 1.39(1) Å). The X-ray analysis revealed the presence of another C_6D_6 crystallization molecule with its gravity center on a crystallographic center of symmetry. The hydrogen atoms, except those related to the solvent molecules of crystallization in **9** and **11**, which were ignored, were located from difference Fourier maps and introduced in the subsequent refinements as fixed atom contribution with *U*'s fixed at 0.08 for **9**, **11**, and **13** and 0.10 Å^2 for **12**. The final difference maps showed no unusual feature, with no significant peak above the general background. The crystal chirality of complex **13**, which crystallizes in a polar space group, was tested by inverting all the coordinates ($x, y, z|-x, -y, -z$) and refining to convergence once again. The resulting *R* values quoted in Table 1 indicated that the original choice should be considered the correct one.

Final atomic coordinates are listed in Tables S2−S5 for non-H atoms and in Tables S6−S9 for hydrogens. Thermal parameters are given in Tables S10−S13, and bond distances and angles, in Tables S14−S17.[24]

Scheme 1

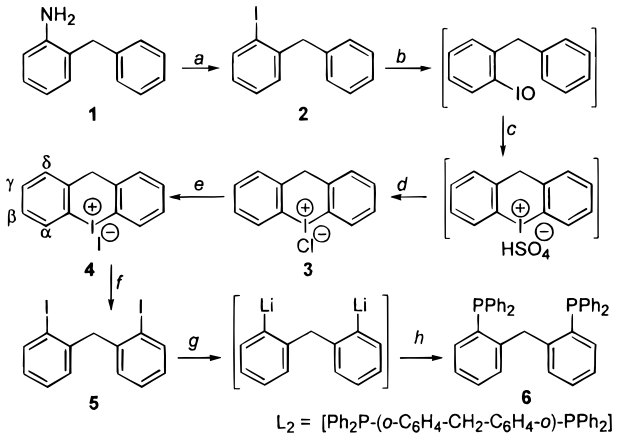

Steps *a*-*h* are reported in detail in the Experimental Section
α, β, γ, δ: numbering scheme for the NMR spectrum

Results and Discussion

The synthesis of our target chelating ligand L_2, **6**, is outlined in Scheme 1. This stepwise synthesis starts from commercially available **1** and involves classic methodologies for the preparation of the intermediates **2**−**5** leading to the diphosphine, **6**. Specific reference to the methods applied, along with a detailed synthesis of each intermediate, has been reported in the Experimental Section. The present strategy has the advantage of being easily scaled to *ca.* 20 g of the target diphosphine. It is worth noting that the last step (*h*) of the sequence (Scheme 1) should in principle allow the generation of a variety of different substituted diphosphines depending on the dialkyl- or diarylchlorophosphine used.

(19) Ugozzoli, F. ABSORB, a Program for F_o Absorption Correction. *Comput. Chem.* **1987**, *11*, 109.
(20) North, A. C. T.; Phillips, D. C.; Mathews, F. S. *Acta Crystallogr., Sect. A: Cryst. Phys., Diffr., Theor. Gen. Crystallogr.* **1968**, *A24*, 351.
(21) (a) *International Tables for X-ray Crystallography*; Kynoch Press: Birmingham, England, 1974; Vol. IV, p 99. (b) *Ibid.*, p 149.
(22) Stewart, R. F.; Davidson, E. R.; Simpson, W. T. *J. Chem. Phys.* **1965**, *42*, 3175.
(23) Sheldrick, G. M. *SHELXL92 Gamma Test: Program for Crystal Structure Refinement*; University of Göttingen: Göttingen, Germany, 1992.

(24) See paragraph at the end regarding Supporting Information.

Scheme 2

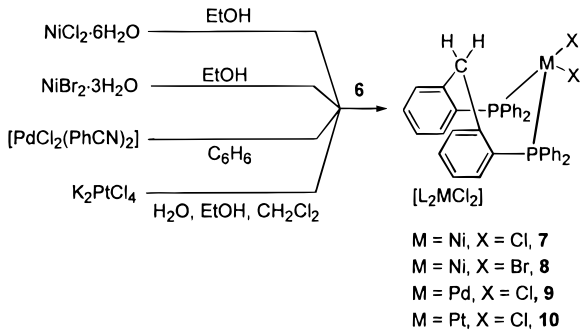

Ligand **6** has been characterized as reported in the Experimental Section. Its $^{31}P\{^1H\}$ NMR spectrum shows a singlet at −11.5 ppm, while the bridging methylene appears as a triplet at 4.45 ppm (J_{P-H}, 2.0 Hz) in the ^1H NMR. It has been engaged in the complexation of some metal fragments which can be considered as prototypes in organometallic chemistry. Their syntheses are reported in Scheme 2.

Although complexes **7** and **8** are useful starting materials, their paramagnetism did not allow an inspection of the ligand's NMR characteristics when bound a metal. The magnetic moment suggests a typical tetrahedral coordination geometry. The NMR spectra of **9** and **10** are, on the contrary, particularly significant. Due to the rather narrow P···P bite angle and the constantly rigid conformation of the metallacycle, we assume that our compounds are exclusively *cis*, not only in the solid state (*vide infra*) but also in solution.[25] In the case of **9**, the $^{31}P\{^1H\}$ NMR spectrum shows a singlet for the two phosphorus atoms at 23.4 ppm, in agreement with a variety of $[(PR_3)_2PdCl_2]$ complexes,[26] while in the case of **10** the signal is a 1:4:1 multiplet at 3.55 ppm, with a $J_{Pt-P} = 3.686$ Hz. Such values should be compared with those of other $PtCl_2$−diphosphine metallacycles containing a bidentate phosphorus ligand in which the two PPh_2 fragments are bridged by an aliphatic chain of variable length.[27] Both values seem to be affected, without showing a regular trend, by the size of the metallacycle, unlike previous observations for the smaller metallacycles.[28] The ^1H NMR spectrum for both **9** and **10** shows clearly differentiated *exo* and *endo* protons of the bridging methylene. The two protons become, in fact, diastereotopic on complexation. The *endo* proton (complex **9**) gives rise to a doublet of triplets at 6.45 ppm, due both to the geminal and phosphorus coupling (J_{HH}, 14 Hz; J_{PH}, 3.0 Hz), while in the case of **10** the *endo* proton (6.46 ppm) appears as a broad doublet due to the barely detectable P−H coupling. The *exo* proton is a doublet at 3.84 ppm (J_{H-H}, 14 Hz, **9**) and 3.44 (J_{H-H}, 14 Hz, **10**). The difference in chemical shift between the pair of doublets arising from the $-CH_2-$ moiety in the complexed form of the ligand is particularly sensitive to the nature of the metal, its coordination number, or in general its chemical environment. One of the explanations which can be invoked may be the geometrical proximity, i.e., a long-range interaction between the *endo* proton and the metal. The X-ray analysis of **9** is particularly informative in this sense. The metal has the distorted square planar geometry shown in Figure 1.

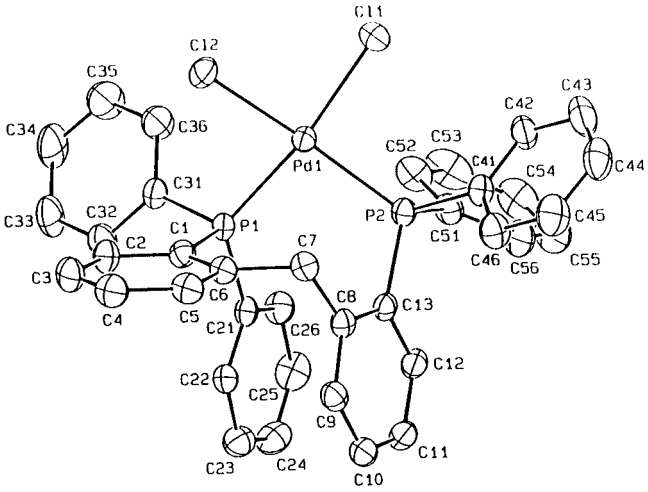

Figure 1. ORTEP drawing of complex **9** (30% probability ellipsoids).

Table 2. Selected Bond Distances (Å) and Angles (deg) for Complex **9**

Pd1−Cl2	2.360(1)	P1−C31	1.840(5)
Pd1−P1	2.271(1)	P2−C13	1.828(5)
Pd1−P2	2.268(1)	P2−C41	1.833(4)
P1−C1	1.823(5)	P2−C51	1.814(5)
P1−Pd1−P2	96.4(1)	C21−P1−C31	97.9(2)
Cl2−Pd1−P2	165.8(1)	C1−P1−C31	110.1(2)
Cl2−Pd1−P1	84.6(1)	C1−P1−C21	105.8(2)
Cl1−Pd1−P2	91.0(1)	Pd1−P2−C51	114.1(2)
Cl1−Pd1−P1	170.7(1)	Pd1−P2−C41	116.1(2)
Cl1−Pd1−Cl2	89.5(1)	Pd1−P2−C13	112.3(2)
Pd1−P1−C31	111.6(2)	C41−P2−C51	101.4(2)
Pd1−P1−C21	123.7(2)	C13−P2−C51	109.4(2)
Pd1−P1−C1	107.0(1)	C13−P2−C41	102.6(2)

The distortion is mainly indicated by the Cl2−Pd−P2 bond angle [165.8(1)°] (Table 2) and the tetrahedral displacements of the atoms from the mean coordination plane: Pd1, 0.018(1); Cl1, 0.145(2); Cl2, −0.271(2); P1, 0.149(2); P2, −0.265(2) Å. The chelating behavior of the ligand results in an eight-membered chelation ring which assumes a distorted *boat*−*boat* conformation (Figure 5a), the P1, C1, C8, and C13 atoms defining the basal plane (maximum displacement 0.007(5) Å for C8). The angle formed by the almost parallel C8−C13 and P1−C1 bonds is 8.7(3)°. This feature of the metallacycle could be described, considering the C1−C6−C7−C8 [−67.1(6)°] and P1−Pd1−P2−C13 [−30.2(2)°], by the torsion angles which should be equal to zero in a nondistorted *boat*−*boat* conformation. It is worth noting that the value of the first torsion angle is comparable with those in complexes **11** and **12** (*vide infra*) (−80.4(8) and −74.6(5)°, respectively), while the value of the latter indicates a deformation larger than that in complexes **11** and **12** where the P1−Pd1−P2−C13 torsion angle is 2.7(2) and −3.9(1)°, respectively. The conformation of the metallacycle is such as to orient the H71 hydrogen atom almost perpendicular to the coordination plane (Pd···H71, 2.46 Å), the angle between the Pd1···H71 line and the normal to the plane being 19.1(3)°. The P1···P2 bite distance is 3.385(2) Å. The phenyl rings of the ligand **6** adopt a conformation which results in a pair of hydrogen atoms (H36, H52) of different rings capping the metal (Pd1···H36, 2.77; Pd1···H52, 2.89 Å) on the opposite side with respect to H71. The plane through Pd1, H36, and H52 forms a dihedral angle of 82.9° with the coordination plane. In spite of different coordination geometries in complexes **9**, **11**, and **12** the mutual orientation of the C1···C6 (Ph1) and C8···C13 (Ph2) aromatic rings does not vary remarkably, as indicated by the values of the dihedral angle between Ph1 and Ph2 [81.4(2), 76.6(2), and 77.8(2)° for **9**, **11**, and **12**, respectively] and the

(25) In all the metallacycles derived from the same skeleton, regardless of the nature of the donor atom O,[6] N,[29] and P *cis* compounds have been exclusively obtained.

(26) (a) Meek, D. W.; Nicpon, P. E.; Imhof Meek, V. *J. Am. Chem. Soc.* **1970**, *92*, 5351. b) *Phosphorus-31 NMR Spectroscopy in Stereochemical Analysis*; Verkade, J. G., Quin, L. D., Eds.; VCH: Weinheim, Germany, 1987.
(27) Lindner, E.; Fawzi, R.; Mayer, H. A.; Eichele, K.; Hiller, W. *Organometallics* **1992**, *10*, 1033.
(28) Garrou, P. E.; *Chem. Rev.* **1981**, *81*, 229.

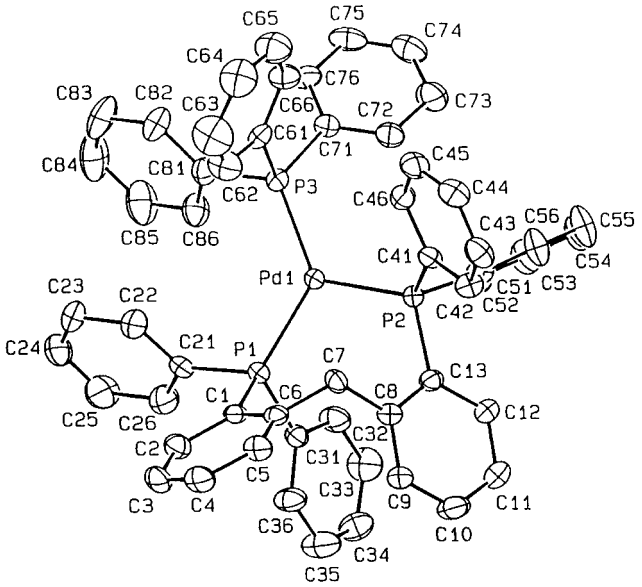

Figure 2. ORTEP drawing of complex **11** (30% probability ellipsoids).

Scheme 3

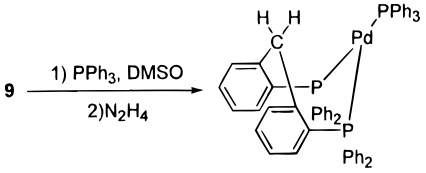

[$L_2Pd(PPh_3)$], **11**

C5−C6−C8−C9 torsion angle [40.1(6), 45.4(7), and 40.8(4)° for **9**, **11**, and **12**, respectively] which reflects the bending and the twisting of the two rings. Similar structural parameters have been observed in the structure of **10**.[29]

Complex **9** has been engaged in a number of transformations, demonstrating its utility as a starting material. Reduction with hydrazine in the presence of PPh_3 gave the tricoordinated Pd^0 derivative **11** (Scheme 3).[30]

The $^{31}P\{^1H\}$ NMR spectrum of **11** shows two singlets at 23.9 and 6.8 ppm for the phosphorus set, the first one belonging to the bidentate phosphine. It may be that the hydrogens from the bridging methylene play a particular role, protecting the coordinative unsaturation of the metal, as suggested by the structure of **11**, shown in Figure 2.

Palladium is trigonally coordinated to the phosphorus donor atoms and the out-of-plane distance from the P_3 plane is 0.046(1) Å. The Pd−P1 [2.328(2) Å] and Pd−P2 [2.324(2) Å] bond distances are in good agreement with the values reported in the literature for Pd(0)−PPh_3 bonds *e.g.* 2.316(5) Å in [Pd-$(PPh_3)_3$].[31,32] They are significantly longer than those observed in the Pd(II) square planar complex **9**. The eight-membered chelate ring assumes a *boat*−*boat* conformation (Figure 5b); the angle between the P1−C1 and C8−C13 bonds defining the basal plane [26.4(4)°] is remarkably wider than that found in **9**. The Pd···H71 contact is 2.61 Å, the angle between the Pd1···H71 line with the normal to the co-ordination plane being 41.6°. No other intramolecular Pd···H contacts shorter than 3.02 Å are observed. The P1···P2 bite distance [3.847(2) Å] is rather wide, due to the trigonal coordination of the metal. In the ^1H NMR spectrum of **11**, the resonances of *endo* and *exo* protons ($\Delta = 3.07$ ppm) are clearly separated and give rise to two distinct pairs of doublets ($J_{H-H} = 14$ Hz), though the coupling of the *endo* one can be missed because of the rather broad shape of the peaks. The C···H···M interaction mentioned above is structurally or spectroscopically detectable only when the C−H bond is kept in a fixed position close to the metal, reflecting the rigid overall conformation of the molecule.[33]

Table 3. Selected Bond Distances (Å) and Angles (deg) for Complex **11**

Pd1−P1	2.328(2)	P2−C13	1.845(5)
Pd1−P2	2.324(2)	P2−C41	1.838(5)
Pd1−P3	2.289(2)	P2−C51	1.831(6)
P1−C1	1.854(6)	P3−C61	1.819(8)
P1−C21	1.824(6)	P3−C71	1.838(6)
P1−C31	1.828(7)	P3−C81	1.845(6)
P2−Pd1−P3	122.6(1)	Pd1−P2−C13	113.0(2)
P1−Pd1−P3	125.7(1)	C41−P2−C51	101.2(3)
P1−Pd1−P2	111.6(1)	C13−P2−C51	103.9(3)
Pd1−P1−C31	113.6(2)	C13−P2−C41	102.4(2)
Pd1−P1−C21	114.8(2)	Pd1−P3−C81	120.7(3)
Pd1−P1−C1	122.0(2)	Pd1−P3−C71	118.6(2)
C21−P1−C31	101.5(3)	Pd1−P3−C61	109.2(2)
C1−P1−C31	102.0(3)	C71−P3−C81	100.0(3)
C1−P1−C21	100.0(3)	C61−P3−C81	103.1(3)
Pd1−P2−C51	119.7(2)	C61−P3−C71	102.9(3)
Pd1−P2−C41	114.5(2)		

Scheme 4

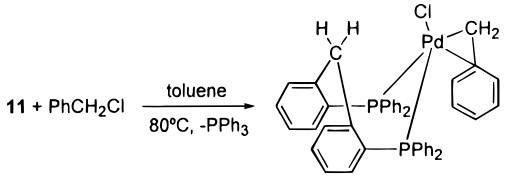

[$L_2Pd(Cl)(\eta^2\text{-}CH_2Ph)$], **12**

Complex **11** can be a particularly useful source of Pd(0) for making Pd−C bonds *via* oxidative addition reactions.[34] One of them is reported in Scheme 4.

The reaction with benzyl chloride led to the synthesis of a η^2-monobenzyl derivative.[35] The $^{31}P\{^1H\}$ NMR spectrum displays two singlets at 9.6 and 27.7 ppm, while the ^1H NMR spectrum of the bridging methylene shows a doublet for the H_{exo} at 3.25 ppm, with the resonances of the H_{endo} overlapping

(29) Floriani, C.; Chiesi-Villa, A.; Rizzoli, C. Unpublished results.
(30) (a) Malatesta, L.; Angoletta, M. *J. Chem. Soc.* **1952**, 1186. (b) Coulson, D. R. *Inorg. Synth.* **1972**, *13*, 21. (c) Dobinson, G. C.; Mason, R.; Robertson, G. B.; Ugo, R.; Conti, F.; Morelli, D.; Cenini, S.; Bonati, F. *J. Chem. Soc., Chem. Commun.* **1967**, 739. (d) Clemmit, A. F.; Glockling, F. *J. Chem. Soc. A* **1969**, 2163.
(31) Sergienko, V. S.; Porai-Koshits, M. A. *Zh. Strukt. Khim.* **1987**, *28*, 103.
(32) Orpen, A. G.; Brammer, L.; Allen, F. H.; Kennard, O.; Watson, D. G.; Taylor, R. *J. Chem. Soc., Dalton Trans.* **1989**, S1.
(33) (a) Crabtree, R. H.; Hamilton, D. G. *Adv. Organomet. Chem.* **1988**, *28*, 299. (b) Crabtree, R. H. *Angew. Chem., Int. Ed. Engl.* **1993**, *32*, 789 and references therein. (c) Brookhart, M.; Green, M. L. H. *J. Organomet. Chem.* **1983**, *250*, 395. (d) Brookhart, M.; Green, M. L. H.; Wong, L. L. *Prog. Inorg. Chem.* **1988**, *36*, 1. (e) Kretz, C. M.; Gallo, E.; Solari, E.; Floriani, C.; Chiesi-Villa, A.; Rizzoli, C. *J. Am. Chem. Soc.* **1994**, *116*, 10775.
(34) (a) Canty, A. J. In *Comprehensive Organometallic Chemistry II*; Abel, E. W., Stone, F. G. A., Wilkinson, G., Eds.; Pergamon: Oxford, U.K., 1995; Vol. 9, Chapter 5. (b) Stille, J. K. In *The Chemistry of the Metal-Carbon Bond*; Hartley, F. R., Patai, S., Eds.; Wiley: New York, 1985; Vol. 2, p 625.
(35) (a) Dryden, N. H.; Legzdins, P.; Trotter, J.; Yee, V. C. *Organometallics* **1991**, *10*, 2857. (b) Solan, G. A.; Cozzi, P. G.; Floriani, C.; Chiesi-Villa, A.; Rizzoli, C. *Organometallics* **1994**, *13*, 2572. (c) Pellecchia, C.; Grassi, A.; Immirzi, A. *J. Am. Chem. Soc.* **1993**, *115*, 1160. (d) Kalinin, V. N.; Cherepanov, I. A.; Moiseev, S. K.; Batsanov, A. S.; Struchkov, Yu. T. *Mendeleev Commun.* **1991**, 77. (e) Jordan, R. F.; LaPointe, R. E.; Baenziger, N.; Hinch, G. D. *Organometallics* **1990**, *9*, 1539. (f) Canty, A. J.; Traill, P. R.; Skelton, B. W.; White, A. H. *J. Organomet. Chem.* **1992**, *433*, 213.

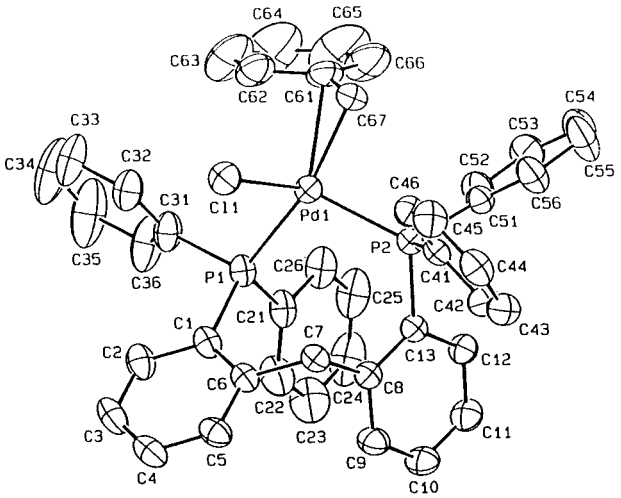

Figure 3. ORTEP drawing of complex **12** (30% probability ellipsoids).

Table 4. Selected Bond Distances (Å) and Angles (deg) for Complex **12**

Pd1−Cl1	2.541(2)	P1−C21	1.833(5)
Pd1−P1	2.383(1)	P1−C31	1.830(4)
Pd1−P2	2.259(1)	P2−C13	1.830(4)
Pd1−C61	2.408(6)	P2−C41	1.838(4)
Pd1−C67	2.113(6)	P2−C51	1.822(3)
P1−C1	1.838(4)		
C61−Pd1−C67	36.4(2)	Pd1−P1−C21	114.7(1)
P2−Pd1−C67	90.2(1)	Pd1−P1−C1	120.2(1)
P2−Pd1−C61	109.1(1)	C21−P1−C31	102.2(2)
P1−Pd1−C67	161.9(1)	C1−P1−C31	102.3(2)
P1−Pd1−C61	126.0(1)	C1−P1−C21	104.6(2)
P1−Pd1−P2	103.2(1)	Pd1−P2−C51	115.7(1)
Cl1−Pd1−C67	89.9(1)	Pd1−P2−C41	112.5(1)
Cl1−Pd1−C61	103.1(1)	Pd1−P2−C13	115.4(1)
Cl1−Pd1−P2	124.1(1)	C41−P2−C51	104.1(2)
Cl1−Pd1−P1	92.6(1)	C13−P2−C51	105.6(2)
Pd1−P1−C31	110.7(1)	C13−P2−C41	101.9(2)

those of the aromatic protons. The η^2-bonding mode of the benzyl group has been revealed by the ^{1}H NMR spectrum with the presence of a pair of unresolved doublets for the two heterotopic benzylic protons (see Experimental Section)[35] and confirmed by an X-ray analysis of **12** (Figure 3).

The structure consists of the packing of **12** and toluene solvent molecules of crystallization in the molar ratio of 1/1. Selected bond distances and angles are listed in Table 4. The range of the palladium−carbon distances suggests a metal−benzyl η^2-bonding mode involving the C61 and C67 carbon atoms [Pd1−C67, 2.113(6) Å; Pd1−C61, 2.408(6)], the Pd1−C62, 2.729(6), and Pd-C66, 3.315(6) Å, being too long to be considered as interactions. The presence of a η^2-interaction instead of a σ-bond is supported by the value of the Pd−C67 distance, though significantly longer than those observed for Pd−C σ-bonds [mean value 2.064(14) Å][36] and by the value of the Pd1−C67−C61 angle [83.0(4)°] which differs remarkably from the tetrahedral one. The Pd1−P2 [2.259(1) Å] bond distance is close to those observed in complex **9**, while the Pd1−P1 [2.383(1) Å] as well as the Pd1−Cl1 [2.541(2) Å] bond distances are remarkably longer. This lengthening could be attributed to intraligand steric hindrance rather than to electronic effects, as indicated by the P1···Cl1 [3.560(2) Å] and C67−Cl1 [3.301(5) Å] contacts which nearly correspond to the sum

Scheme 5

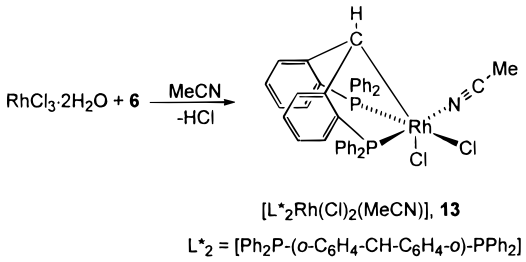

[L*$_2$Rh(Cl)$_2$(MeCN)], **13**

L*$_2$ = [Ph$_2$P-(*o*-C$_6$H$_4$-CH-C$_6$H$_4$-*o*)-PPh$_2$]

of the respective van der Waals radii. The conformation of the chelation ring is close to that observed in **11** (Figure 5c). The angle formed by the P1−C1 and C8−C13 bonds defining the basal plane is 18.2(2)°. The value of the P1···P2 bite distance [3.638(2) Å] is intermediate between those observed in **9** and **11**. The conformation of the metallacycle allows the H71 hydrogen to approach the palladium metal at a distance of 2.77 Å.

The question arising at this stage is the following: Can we force the bridging methylene to play, besides its role as a spectroscopic probe, a chemical role? It is well-known that intramolecular C−H bond activation can be the intermediate step in the intermolecular hydrocarbon activation.[5] The reaction to test this possibility concerns **6** with $RhCl_3$ shown in Scheme 5. It reports an electrophilic attack[37] by Rh(III) on the bridging methylene.

This reaction was carried out in acetonitrile which functions as a base in case of HCl formation. The electrophilic attack of Rh(III) on the bridging methylene is assisted by the close proximity, imposed by the rigid boat−boat conformation of the metallacycle, between the metal and the H_{endo}. Complex **13** has been isolated in high yields as deep yellow crystals. The acetonitrile molecule is only loosely bonded to the metal and is lost under vacuum (see Experimental Section). NMR spectra have been recorded on the desolvated form. The metalated carbon appears as a doublet in the ^{13}C NMR spectrum at 57.28 ppm, with a corresponding J_{Rh-C} coupling constant of 22.4 Hz.[38] In the ^{31}P{^{1}H} NMR spectrum we observe two doublets at 60.3 ppm (J_{Rh-P} = 145 Hz) and 54.6 (J_{Rh-P} = 134 Hz). Such coupling constants are in accordance with the presence of a five-coordinate Rh in the desolvated form.[39] The *exo* proton of the bridging methylene is not particularly informative since it falls in the crowded aromatic region, between 7.1 and 7.8 ppm. The X-ray analysis of **13** has been carried out on its solvated form (Figure 4, Table 5).

The metal shows a slightly distorted octahedral coordination provided by the P1, P2, and C7 atoms from **6**, two chlorine atoms, and the nitrogen atom of an acetonitrile molecule. This distortion is mainly due to the trischelating nature of the ligand which displays a *fac* arrangement around the metal (P1−Rh−P2, 97.7(1)°). The resulting two five-membered chelate rings are nearly perpendicular to each other [dihedral angle between their mean planes, 84.1(1)°], one (Rh1,P2,C13,C8,C7) which is planar and the other (Rh1,P1,C1,C6,C7) folded by 35.0(2)° along the P1···C7 line. This folding is probably due to the sp^3 character of the C7 carbon atom and the *fac* arrangement of

(36) (a) Geib, S. J.; Rheingold, A. L. *Acta Crystallogr. Sect. C* **1987**, *43*, 1427. (b) Osakada, K.; Ozawa, Y.; Yamamoto, A. *J. Chem. Soc., Dalton Trans.* **1991**, 759. (c) Osakada, K.; Ozawa, Y.; Yamamoto, A. *Bull. Chem. Soc. Jpn.* **1991**, *64*, 2002. (d) Reger, D. L.; Garza, D. G.; Lebioda, L. *Organometallics* **1991**, *10*, 902.

(37) (a) Shilov, A. E. *The Activation of Saturated Hydrocarbons by Transition Metal Complexes*; Reidel: Dordrecht, The Netherlands. 1984. (b) Labinger, J. A.; Herring, A. M.; Bercaw, J. E. *Adv. Chem. Ser.* **1992**, *No. 230*, 221. Luinstra, G. A.; Labinger, J. A.; Bercaw, J. E. *J. Am. Chem. Soc.* **1993**, *115*, 3004. (c) Periana, R. *Science* **1993**, *259*, 340.

(38) Mann, B. E.; Taylor, B. F. *13-C NMR Data of Organometallic Compounds*; Academic: New York, 1981; p 44.

(39) Pregosin, P. R.; Kunz, R. W. In *NMR Basic Principles and Progress*; Springer: Berlin, 1979; Vol. 16.

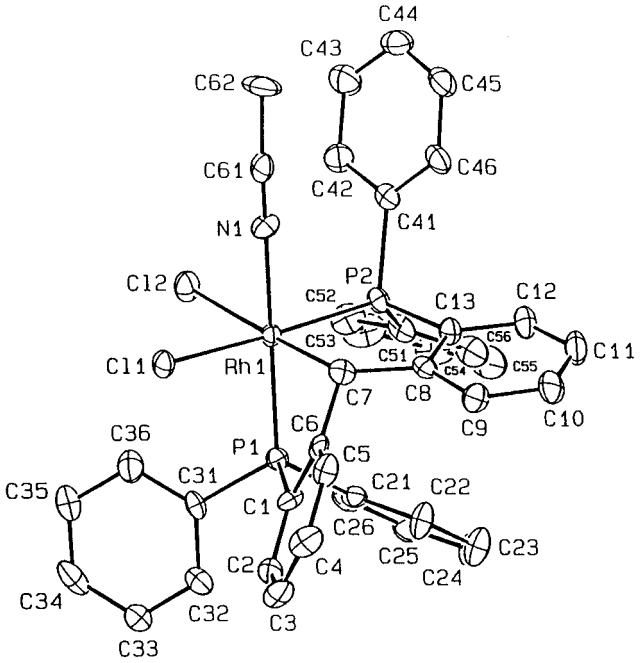

Figure 4. ORTEP drawing of complex **13** (30% probability ellipsoids).

Table 5. Selected Bond Distances (Å) and Angles (deg) for Complex **13**

Rh1−Cl1	2.419(2)	P1−C1	1.807(9)
Rh1−Cl2	2.473(3)	P1−C21	1.827(8)
Rh1−P1	2.265(2)	P1−C31	1.825(9)
Rh1−P2	2.252(2)	P2−C13	1.828(9)
Rh1−N1	2.107(6)	P2−C41	1.853(8)
Rh1−C7	2.108(7)	P2−C51	1.831(9)
N1−Rh1−C7	90.5(3)	Rh1−P1−C31	119.9(3)
P2−Rh1−C7	86.3(2)	Rh1−P1−C21	121.2(3)
P2−Rh1−N1	87.3(2)	Rh1−P1−C1	100.9(3)
P1−Rh1−C7	81.4(2)	C21−P1−C31	100.8(4)
P1−Rh1−N1	170.1(2)	C1−P1−C31	106.6(4)
P1−Rh1−P2	97.7(1)	C1−P1−C21	106.2(4)
Cl2−Rh1−C7	176.8(2)	Rh1−P2−C51	123.0(3)
Cl2−Rh1−N1	86.3(2)	Rh1−P2−C41	113.7(3)
Cl2−Rh1−P2	94.3(1)	Rh1−P2−C13	103.2(3)
Cl2−Rh1−P1	101.6(1)	C41−P2−C51	99.4(4)
Cl1−Rh1−C7	88.5(2)	C13−P2−C51	110.5(4)
Cl1−Rh1−N1	86.5(2)	C13−P2−C41	106.1(4)
Cl1−Rh1−P2	171.9(1)	Rh1−N1−C61	174.3(7)
Cl1−Rh1−P1	87.6(1)	N1−C61−C62	175.6(10)
Cl1−Rh1−Cl2	90.5(1)		

the ligand (Figure 5d). Other peculiar features are the C1−C6−C7−C8 torsion angle [−93.3(9)°], the P1···P2 bite distance [3.403(2) Å], and the dihedral angle between the aromatic rings of the ligand [113.0(3)°]. The two Rh−P bond lengths [Rh−P1, 2.265(2); Rh−P2, 2.252(2) Å], as well as the Rh−C7 [2.108(7) Å] bond distance are in agreement with the values observed in the Milstein complex[5a] and metalated Rh(III) species.[40] The relatively high *trans*-influence of the methylenic carbon is shown by the lengthening of Rh−Cl2 [2.473(3) Å] with respect to Rh−Cl1 [2.419(2) Å].

In order to better define the spectroscopic and, eventually, the steric properties of our novel chelating phosphine, we explored its binding ability in some nickel and iron complexes. The reaction in Scheme 6 shows the synthesis of two Ni^0 derivatives with different coordination number at the metal.

The conventional reduction of $[Ni(acac)_2]$ in the presence of C_2H_4[13,41] afforded the very reactive monoethylene−Ni(0) complex, **14**. It has been obtained as a green-yellow crystalline solid. Its relatively high stability depends on the steric protection of the diphosphine ligand which provides a type of protective cage. The easy displacement of C_2H_4 by carbon monoxide led to the tetracoordinate Ni(0)−dicarbonyl derivative **15**.[42] Let us now compare the spectroscopic properties of the ligand in the two cases. The $^{31}P\{^1H\}$ NMR spectrum shows for **14** and **15** singlets at 22.7 (C_6D_6) and 24.8 (CD_2Cl_2) ppm, respectively. The ^1H NMR spectrum shows a doublet for the H_{exo} in **14** at 3.49 ppm, while the H_{endo} overlaps with the ethylene protons in the aromatic region (6.60−7.50 ppm). In the case of **15**, H_{endo} appears as a doublet at 5.91 ppm, while the H_{exo} remains almost unchanged at 3.42 ppm. In the X-ray analysis of **15**[43] we observed the usual structural feature of the metal-bonded ligand **6**, including the metallacycle conformation. These results show how the methylene protons are sensitive to the metal environment. In the meantime we found, however, that they are only slightly sensitive to the solvent used for the NMR spectrum. In all the cases so far reported, we assumed that the eight-membered metallacycle conformation does not change significantly because of the presence of the transition metal and thanks to its size.[25] In order to prove the consequence of the ring size on the spectroscopic behavior of the bridging

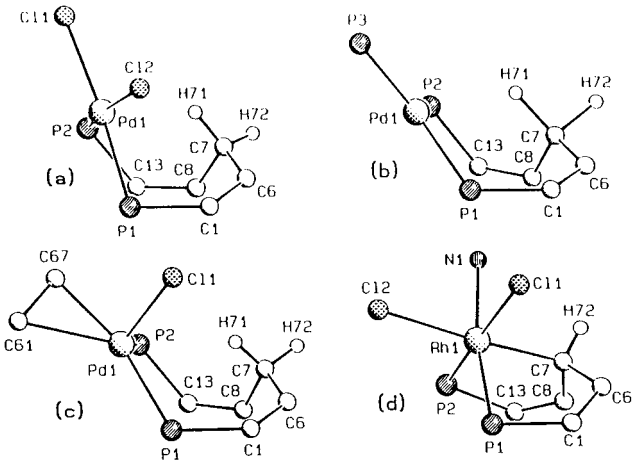

Figure 5. SCHAKAL drawing showing the conformation of the chelation rings in complexes **9** (a), **11** (b), **12** (c), and **13** (d).

Scheme 6

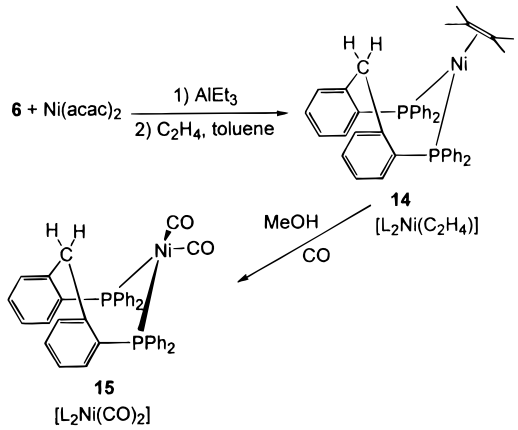

(40) Sharp, P. R. In *Comprehensive Organometallic Chemistry II*; Abel, E. W., Stone, F. G. A., Wilkinson, G., Eds.; Pergamon: Oxford, U.K., 1995; Vol. 8, Chapter 2.

(41) (a) Chatt, J.; Hart, F. A.; Watson, H. R. *J. Chem. Soc.* **1962**, 2537. (b) Aresta, M.; Nobile, C. F.; Sacco, A. *Inorg. Chim. Acta* **1975**, *12*, 167.

(42) Cenini, S.; Ratcliff, B.; Ugo, R. *Gazz. Chim. Ital.* **1974**, *104*, 1161.

(43) Crystal data for **15**: $C_{39}H_{30}NiO_2P_2 \cdot CD_2Cl_2$, $M = 738.3$, triclinic, space group $P\bar{1}$, $a = 13.157(5)$ Å, $b = 14.087(6)$ Å, $c = 11.123(4)$ Å, $\alpha = 112.00(3)°$, $\beta = 106.59(4)°$, $\gamma = 94.13(4)°$, $Z = 2$, $R = 0.045$ ($wR2 = 0.112$).

Scheme 7

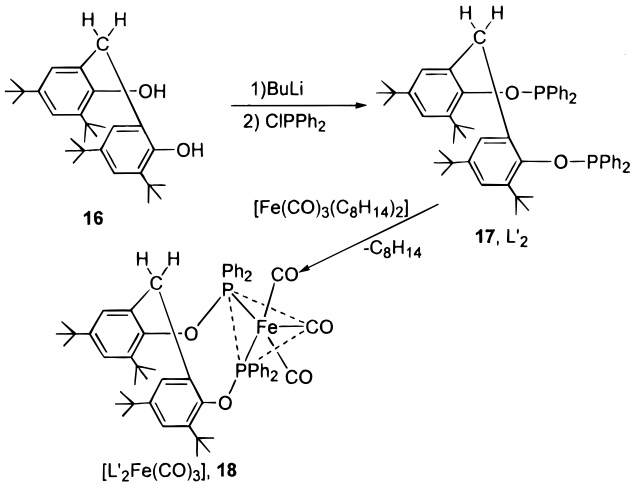

Scheme 8

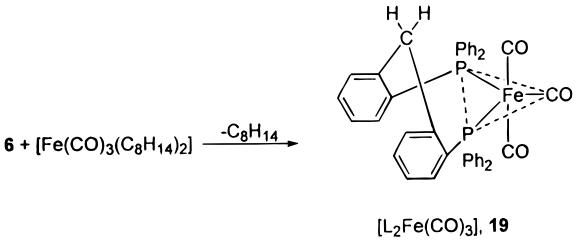

methylene, we prepared the 10-membered metallacycle using the phosphite−phosphine bidentate ligand **17** derived from the same skeleton (Scheme 7).

Ligand **17** has been reacted with $[Fe(CO)_3(C_8H_{14})_2]$[14] to afford **18**. Ligand **17** can display either a bridging or a chelating bonding mode,[4] the latter one being shown in the proposed structure of **18**. The chelate bonding mode of **17**, however, is supported by the X-ray structural determination on the closely related $[L'_2Mo(CO)_3]$.[29] The $^{31}P\{^1H\}$ NMR spectrum shows a singlet at 172.0 ppm, while that of **17** is at 113.5 ppm. The bridging methylene is a poorly defined triplet at 4.09 ppm in the free ligand **17**, while the same triplet is displaced to 3.29 ppm in **18** [J_{P-H} = 11.8 Hz]. According to the geometrical flexibility of the 10-membered metallacycle, the two methylene protons are not differentiated; thus $-CH_2-$ cannot serve as a spectroscopic probe for the metal environment. This is proved by the comparison with complex **19**, where the same $[Fe(CO)_3]$ fragment is bonded to ligand **6** to form an eight-membered metallacycle (Scheme 8).

In the case of **19**, the bridging methylene protons appear as a pair of doublets at 3.28 and 5.83 ppm (J_{H-H} = 14 Hz) and the phosphorus at 56.8 (s) ppm. In both complexes the local symmetry of iron is C_{2v}, with the phosphorus occupying two equatorial sites,[44] which thus gives rise to CO IR-active stretching bands $2A_1 + B_2$ at 2008, 1938, 1915 cm^{-1} (complex **18**) and 1984, 1909, 1890 cm^{-1} (complex **19**).

Concluding Remarks

The use of the specifically designed ligand **6** with a variety of organometallic fragments served to emphasize some of its structural, chemical, and spectroscopic properties. Among them we should mention the following: (1) The steric hindrance along with the weak interaction of the metal with the *endo* hydrogen of the bridging methylene provides a protective cavity for reactive, that is coordinatively unsaturated, metal centers. (2) The close geometrical proximity between the *endo* hydrogen from the bridging methylene and the metal favors metalation, which can play a very peculiar role in the σ-bond metathesis reaction with hydrocarbons, thus promoting intermolecular activation. (3) The rigid conformation of the eight-membered metallacycle allowed the differentiation of the *exo* and *endo* protons. The latter one is able to serve as a spectroscopic probe for structural correlations, particularly considering the changes in chemical shift and the magnitude of the J_{P-H} coupling constant.[26] The first argument concerning this structural spectroscopic relationship is based on geometrical constraints and postulates a sort of weak interaction between the metal center and the H_{endo} proton. However, this kind of interaction was not further specified. An agostic type of interaction can be excluded, because this would result in a high-field shift for the proton which undergoes the agostic interaction.[33c,d] This is clearly not the case. Instead, the opposite trend was observed, a downfield shift of the signal assigned to H_{endo}, compared to the free ligand. This phenomenon may be explained in terms of an increased deshielding of the *endo* proton, because the formation of a metallacycle results in an additional ring current which opposes the external field.[28,45] Additional electron density increases the deshielding and leads to a further downfield shift, compared to the electron-poor derivatives.

Acknowledgment. We thank the "Fonds National Suisse de la Recherche Scientifique" (Bern, Switzerland, Grant No. 20-40268.94) and Ciba Specialty Chemicals (Basel, Switzerland) for financial support.

Supporting Information Available: X-ray crystallographic files, in CIF format, for complexes **9** and **11**−**13** are available on the Internet only. Access information is given on any current masthead page.

IC9700819

(44) (a) Casey, C. P.; Whiteker, G. T.; Campana, C. F.; Powell, D. R. *Inorg. Chem.* **1990**, *29*, 3376. (b) Ittel, S. D.; Tolman, C. A.; Krusic, P. J.; English, A. D.; Jesson, J. P. *Inorg. Chem.* **1978**, *17*, 3432.
(45) Lindner, E. *Adv. Heterocyclic Chem.* **1986**, *39*, 239.